

Investigation of the Effect of Clamping on Residual Stresses and Distortions in Butt-Welded Plates

M. Seyyedian Choobi^{1,*}, M. Haghpanahi¹ and M. Sedighi¹

Abstract. *One major disadvantage of many arc welding processes is welding-induced residual stresses and distortions. The non-uniform heating and cooling during arc welding result in non-uniform expansion and contraction of the weld and surrounding base material, which produces undesirable residual stresses and deformations in the welded joint. A number of methods can be used to control welding-induced distortions. The methods used for controlling welding distortions affect residual stresses and vice versa. One practical method for minimizing welding angular distortions is the use of clamping. In this paper, the effect of clamping and clamp releasing time on welding residual stresses and distortions in the single-pass butt welding of 304 stainless steel plates are investigated. Cases with and without clamping have been studied, and residual stresses and angular distortions have been predicted by three-dimensional finite element simulation. Moreover, experiments have been carried out to measure temperature histories, angular distortions and residual stresses for the unclamped case to verify the numerical model. The results of this study revealed that clamping and clamp release time have a great influence on the distribution of residual stresses and final angular distortions. Using clamping during welding and releasing after cooling to ambient temperature can significantly reduce the amount of final angular distortions.*

Keywords: *Butt-weld; Residual stress; Angular distortion; Clamping; FEM; Experimental measurement.*

INTRODUCTION

One major disadvantage of many arc welding processes is welding-induced residual stresses and distortions. The non-uniform heating and cooling during arc welding result in non-uniform expansion and contraction of the weld and surrounding base material, which produces undesirable residual stresses and deformations in the welded joint. During the past decades, numerous experimental and numerical studies have been conducted to predict welding residual stresses and distortions. For example, Deng and Murakawa [1], Long et al. [2] and Deng [3] investigated welding residual stresses and distortions in thin butt-welded plates using the finite element method. Chang and Teng [4] investigated the two-dimensional behavior of residual stresses in butt-welded carbon steel plates by

finite element simulation and X-ray diffraction measurement. Camilleri et al. [5] and Mollicone et al. [6] predicted welding induced distortions in butt-welded plates using two-dimensional finite element simulation. In a similar work, Bachorski et al. [7] investigated welding distortions in carbon steel plates using the finite element method.

Today, the issue of controlling and reducing welding distortions is one of the major problems in industry. A number of different methods have been discussed to control or reduce welding-induced distortions. For example, Michaleris and Sun [8] and Deo and Michaleris [9] investigated the effect of thermal tensioning on welding distortions. Mochizuki and Toyoda [10] investigated the effect of reverse-side heating on welding distortions. Seyyedian et al. [11] investigated the effect of welding sequence on angular distortions in butt-welded plates. The methods used for controlling welding distortions affect residual stresses and vice versa.

In this paper, the effect of clamping and clamp releasing time on welding angular distortions and residual stresses in single-pass butt-welding of 304 stainless

1. Department of Mechanical Engineering, Iran University of Science and Technology, Tehran, P.O. Box 16846-13114, Iran.

*. Corresponding author. E-mail: mseyyedian@yahoo.com

Received 30 December 2009; received in revised form 11 April 2010; accepted 20 June 2010

steel plates is investigated, using the finite element method. Welding was performed using Gas Tungsten Arc Welding (GTAW) method. Three different cases have been studied. In the first case, the plates are welded freely without using clamps. In the second case, the plates are clamped during welding and hot released immediately after welding. In the third case, the plates are clamped during welding and are released after cooling down to ambient temperature. Three-dimensional finite element simulation has been performed and residual stresses and distortions are obtained. To simulate this process, a user-subroutine is developed by the ANSYS Parametric Design Language (APDL) [12]. Moreover, experiments have been performed to measure temperature histories, residual stress and distortions in the unclamped case to verify the numerical model.

THERMO-MECHANICAL ANALYSIS

In this section, a sequentially coupled thermo-elastic plastic three-dimensional finite element computational procedure is developed to calculate temperature field, residual stresses and distortions. For this purpose, a non-linear transient thermal analysis is performed first. Subsequently, the temperature histories obtained from the thermal analysis are applied as thermal body loads in a non-linear structural analysis to obtain welding residual stresses and distortions.

3D FE Model

The three-dimensional finite element model used in this simulation is shown in Figure 1. Considering the symmetry condition, only one half of the model is selected as the FE model. The finite element meshes used for both thermal and structural analyses are the same, except for the element type. For thermal analysis, an eight-node, first order brick element with temperature degree of freedom at each node is used. For structural analysis, an eight-node, first order brick element with three translational degrees of freedom

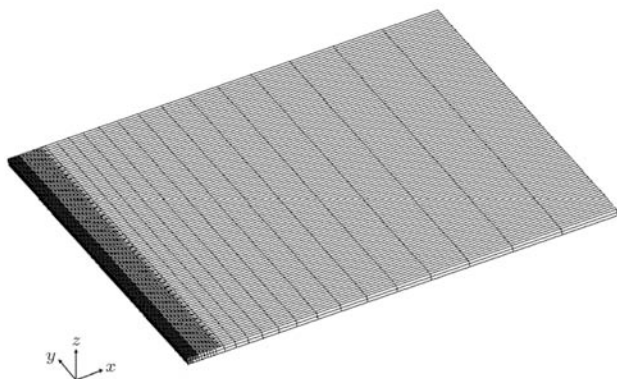


Figure 1. Three-dimensional finite element model.

M. Seyyedian Choobi, M. Haghpanahi and M. Sedighi

at each node is used. Because of high temperature gradients in the Fusion Zone (FZ) and Heat Affected Zone (HAZ), a fine mesh is used within a distance of 10 mm from the weld center line. Away from the HAZ region, the element sizes have increased with the increase of distance from the weld center line.

In the course of the welding process, addition of filler material is modeled using the element birth and death technique. During the thermal analysis, deactivated elements are reactivated sequentially when they come under the influence of the welding torch. For the subsequent structural analysis, birth of an element takes place at the solidification temperature. Melting and ambient temperatures are set as reference temperatures (temperature at which thermal strain is zero) for thermal expansion coefficients of filler and base metals, respectively.

Thermal Analysis

The transient temperature during welding is determined by the three-dimensional nonlinear heat transfer equation:

$$\rho C \frac{\partial T}{\partial t} = \frac{\partial}{\partial X} \left(k \frac{\partial T}{\partial X} \right) + \frac{\partial}{\partial Y} \left(k \frac{\partial T}{\partial Y} \right) + \frac{\partial}{\partial Z} \left(k \frac{\partial T}{\partial Z} \right) + Q, \quad (1)$$

where ρ is density, C is specific heat, k is thermal conductivity, Q is the rate of internal heat generation, T is temperature, t is time, X , Y and Z are coordinates in the reference system. Convection heat transfer with a heat transfer coefficient of $15 \times 10^{-6} \text{ W/mm}^2\text{C}$ is applied to all free surfaces, except the symmetry plane. An adiabatic boundary condition is applied to the symmetry plane. Radiation heat transfer is ignored. In order to consider the heat transfer due to convection stirring in the molten weld pool, an artificially increased thermal conductivity, several times larger than its value at room temperature, was assumed for temperatures above the melting point temperature [13]. Both thermal and mechanical material properties were considered to be temperature-dependent and are given in Table 1. Latent heat is considered 260 J/g between the solidus temperature of 1424°C and the liquidus temperature of 1454°C. Ambient temperature is set to 20°C.

In this study, the heat input from the welding arc is considered as an internal volumetric double-ellipsoid heat source model presented by Goldak [14]. According to the double-ellipsoid model (Figure 2), the power density distribution inside the front and rear quadrants can be expressed by the following equations,

Table 1. Thermal and mechanical material properties of 304 stainless steel.

Temperature (°C)	Conductivity (J/mm°Csec)	Density (g/mm ³)	Specific Heat (J/g°C)	Young's Modulus (GPa)	Yield Stress (MPa)	Poisson's Ratio	Thermal Expansion Coefficient (°C ⁻¹)
0	0.0146	0.00790	0.462	198.50	265.00	0.294	1.70e-5
100	0.0151	0.00788	0.496	193.00	218.00	0.295	1.74e-5
200	0.0161	0.00783	0.512	185.00	186.00	0.301	1.80e-5
300	0.0179	0.00779	0.525	176.00	170.00	0.310	1.86e-5
400	0.0180	0.00775	0.540	167.00	155.00	0.318	1.91e-5
600	0.0208	0.00766	0.577	159.00	149.00	0.326	1.96e-5
800	0.0239	0.00756	0.604	151.00	91.00	0.333	2.02e-5
1200	0.0322	0.00737	0.676	60.00	25.00	0.339	2.07e-5
1300	0.0337	0.00732	0.692	20.00	21.00	0.342	2.11e-5
1500	0.120	0.00732	0.935	10.00	10.00	0.388	2.16e-5

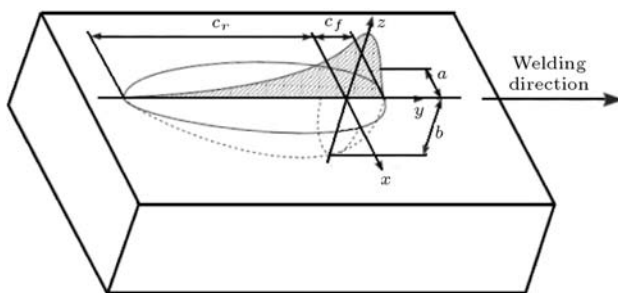


Figure 2. Double-ellipsoid heat source model [14].

respectively:

$$q_f(x, y, z) = \frac{6\sqrt{3}f_f Q}{abc_f \pi^{3/2}} e^{(-3x^2/a^2)} e^{(-3y^2/c_f^2)} e^{(-3z^2/b^2)}, \quad (2)$$

$$q_r(x, y, z) = \frac{6\sqrt{3}f_r Q}{abc_r \pi^{3/2}} e^{(-3x^2/a^2)} e^{(-3y^2/c_r^2)} e^{(-3z^2/b^2)}, \quad (3)$$

where x , y and z are local coordinates attached to the welding heat source, a , b , c_f and c_r are fusion zone dimensions, and f_f and f_r are fractions of heat deposited in the front and rear quadrants, respectively ($f_f + f_r = 2$). The values of heat source parameters are given in Table 2. The variable, Q , which is the heat input per unit time, is given by:

$$Q = \eta UI, \quad (4)$$

where η is welding arc efficiency, U is voltage and I is current. The arc efficiency of the GTAW process is a value between 50%-70% [15]. In this study, arc efficiency is considered 60% to obtain the most correspondence between the numerical and experimental results.

Table 2. Heat source parameters.

Parameters	Value
a	4
b	3
c_f	7
c_r	3
f_f	1.4
f_r	0.6

Mechanical Analysis

Mechanical analysis is carried out using the temperature histories obtained from the thermal analysis. The thermo-elastic-plastic material model based on von Mises yield criterion and kinematic strain hardening rule, which can model the Baushinger effect, is used in this study [16]. For applying boundary conditions, the symmetry plane is fixed in the direction perpendicular to the weld line. The other mechanical boundary conditions are applied at the weld start and stop locations to avoid the rigid body motions of the plate. In cases of using clamps, the free edge of the plate is also fixed in the direction perpendicular to the plate surface. The boundary conditions used for the two welding cases (with and without clamping) are shown in Figure 3.

EXPERIMENTAL VALIDATION

In this part, experiments have been conducted to find out temperature histories, angular distortions and residual stresses for the unclamped case. For this purpose, thin 304 stainless steel plates with dimensions $150 \times 200 \times 2$ mm were single-pass butt-welded using

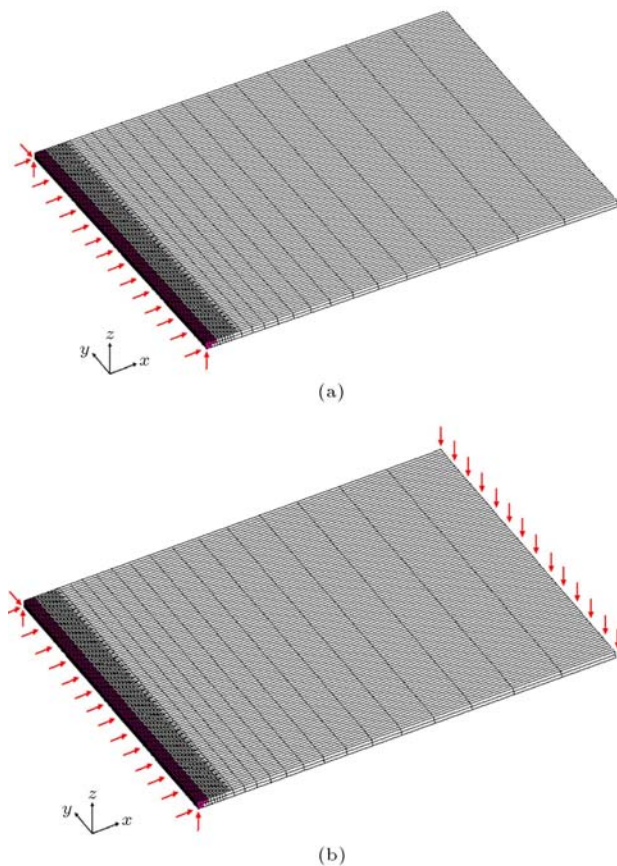


Figure 3. Schematic of boundary conditions on FE model: (a) unclamped case, (b) clamped case.

the GTAW method. The plates had a square-butt groove with zero gaps between parts. Welding was performed with welding current 96 Amp, voltage 10 volt and welding speed of 2.5 mm/sec.

Temperature Measurement

Temperatures were measured using thermocouples of type *K* and thermo meters of type TMC 101. For this purpose, two thermocouples were attached to the top surface at 10 and 20 mm distances from the weld centerline along the mid-section of the plate. During the experiment, most parts of the top and bottom surfaces of the plates were exposed to ambient temperature and the thermocouple joints were protected from heating due to arc radiation.

Angular Distortion Measurement

Deflections have been measured using a mechanical dial gauge. Measurements have been performed at several points at the surface of the plate before and after welding. The measurements have been repeated two times for both left and right sides of the welded plate. The locations of deflection measurements are shown in Figure 4.

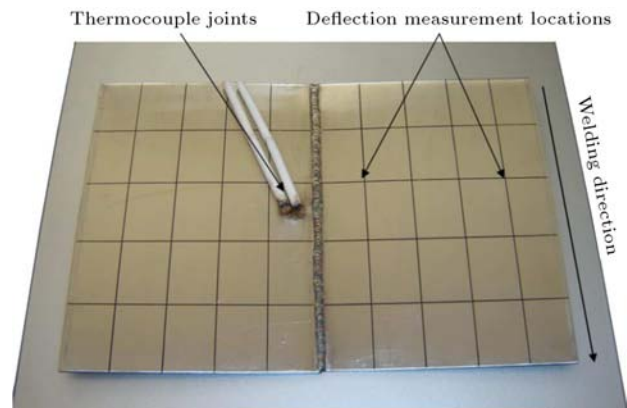


Figure 4. Locations of thermocouples and deflection measurement.

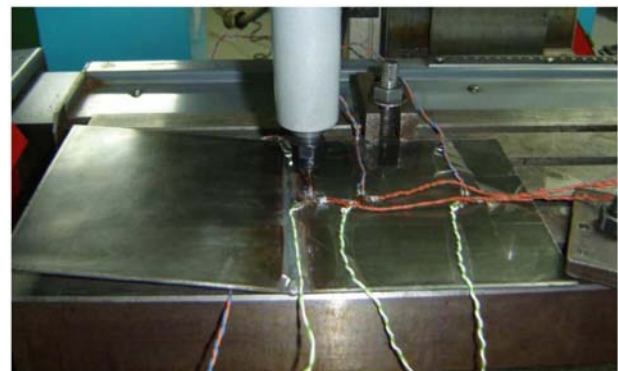


Figure 5. Hole-drilling residual stress measurement set up.

Residual Stress Measurement

Residual stresses have been measured for plates with dimensions $140 \times 150 \times 2$ mm in a previous work of the present authors, using hole-drilling strain gauge method [17]. The hole-drilling experimental set up is shown in Figure 5. Three rosette strain gauges of type *A* were mounted at the top surface of the plate at distances 10, 40 and 100 mm from the weld centerline along the mid-section of the plate. The released strains were measured after drilling in the center point of the gauges using a very high speed drill. The measurements have been repeated two times for each point. More details of the hole-drilling method can be found in ASTM E837 [18].

RESULTS AND DISCUSSION

Figure 6 shows the temperature history results for two measured points at distances 10 and 20 mm from the weld centerline. The numerical results agree well with the experimental measurements. A comparison of finite element and experimentally measured angular distortion results is shown in Figure 7. Deflection measurements have been performed for both right

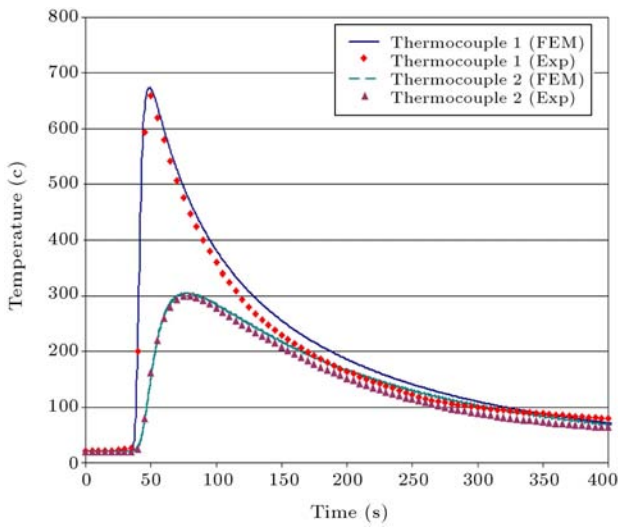


Figure 6. Finite element and experimentally measured temperature histories.

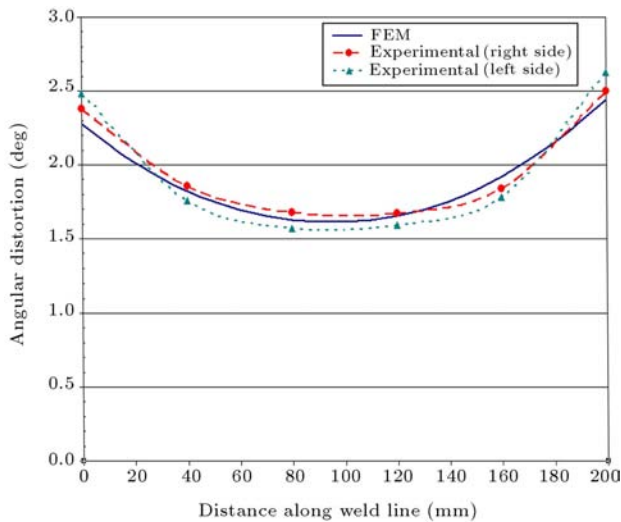


Figure 7. Finite element and experimentally measured angular distortions.

and left sides of the plate. The results show that maximum deflection occurs at the weld stop location where minimum deflection occurs at the mid-length of the weld. The numerical results are in agreement with experimental measurements. The comparison of finite element results with experimental measurements for longitudinal residual stress is shown in Figure 8. The results show that tensile residual stress near the weld region changes to compressive stress and approaches to zero with the distance from the weld centerline.

Figure 9 shows the variation of transverse residual stresses along the weld centerline at the top and bottom surfaces of the plate for three welding cases. The results of transverse residual stresses at the top surface (Figure 9a) show that in the unclamped and clamped hot released cases, the distributions of transverse residual stresses are similar, and they are tensile along the weld

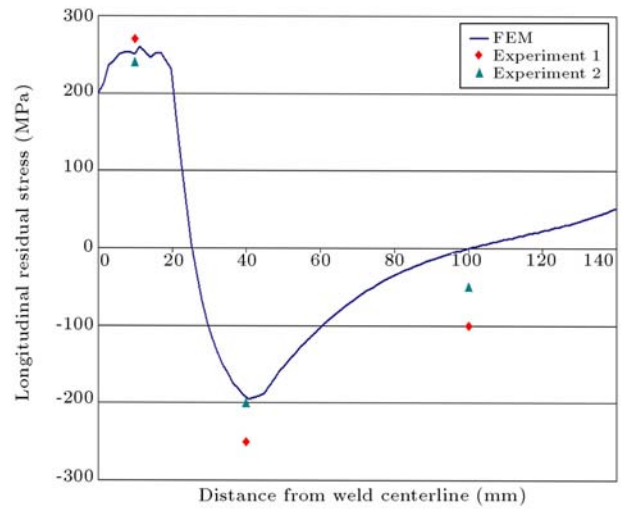
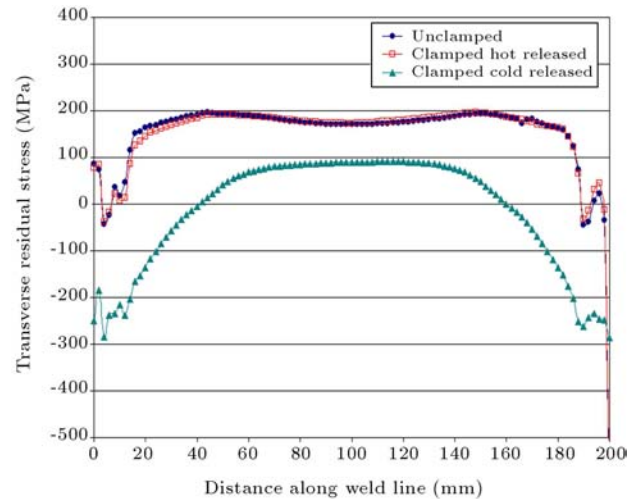
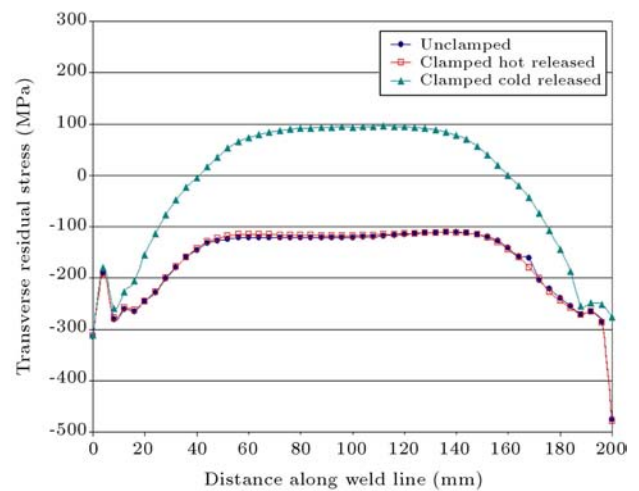


Figure 8. Finite element and experimentally measured longitudinal residual stress.



(a)



(b)

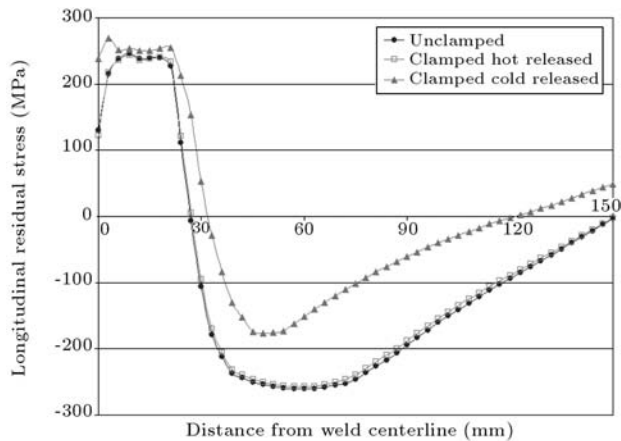
Figure 9. Comparison of transverse residual stresses at (a) top surface and (b) bottom surface.

line. But in the clamped cold released case, transverse residual stresses are compressive at weld start and stop locations, and they are tensile at the middle part of the weld line. The results of transverse residual stresses at the bottom surface (Figure 9b) show that in the unclamped and clamped hot released cases, the distributions of transverse residual stresses are similar and they are compressive along the weld line. But, in clamped cold released case, transverse residual stresses are compressive at the weld start and stop locations, and they are tensile at the middle part of the weld line. The results indicate that in clamped cold released case, the distributions of transverse residual stresses at the top and bottom surfaces are similar, and their values increase in comparison to the unclamped and clamped hot released cases.

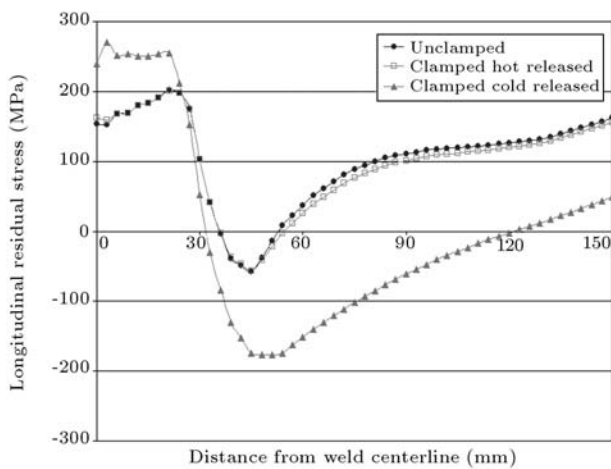
Figure 10 shows the variation of longitudinal residual stresses at the mid-length of the weld, in the direction perpendicular to the weld line, at the top and bottom surfaces of the plate, for three welding cases. The results of longitudinal residual stresses at the

top surface (Figure 10a) show that in the unclamped and clamped hot released cases, the distributions of longitudinal residual stresses are similar. However, in clamped cold released case, the tensile part of the longitudinal residual stress increases in comparison to the unclamped and clamped hot released cases, but the compressive part of the longitudinal residual stress decreases in comparison to the unclamped and clamped hot released cases. The results of longitudinal residual stresses at the bottom surface (Figure 10b) show that in unclamped and clamped hot released cases, the distributions of longitudinal residual stresses are similar. But, in clamped cold released case, the tensile and compressive parts of the longitudinal residual stress increase in comparison to unclamped and clamped hot released cases. The results indicate that in the clamped cold released case, the distributions of longitudinal residual stresses at the top and bottom surfaces are similar.

Figures 11a and 11b show a comparison of the deflection of the plate at the weld start location and

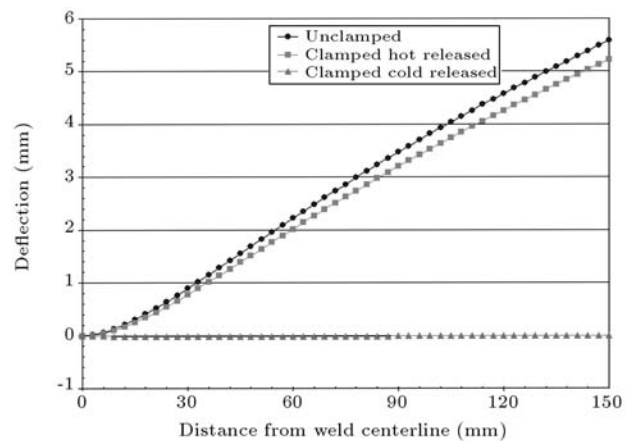


(a)

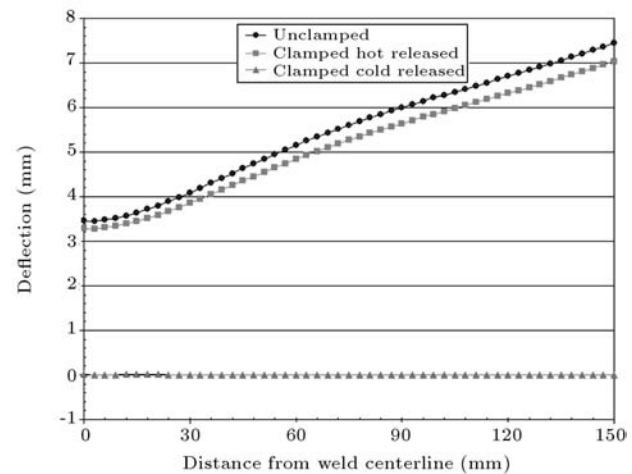


(b)

Figure 10. Comparison of longitudinal residual stresses at (a) top surface and (b) bottom surface.



(a)



(b)

Figure 11. Comparison of deflections at (a) weld start location and (b) middle of the weld line.

at the middle of the weld line, respectively. The results show that clamping reduces angular distortions. A comparison of deflections in the unclamped and clamped hot released cases shows that the deflection of the clamped hot released case is about 0.2 mm less than the deflection of the unclamped case. But, in the clamped cold released case, the deflection reduces significantly to zero.

CONCLUSION

In this paper, the effect of clamping and clamp releasing time on welding residual stresses and angular distortions are investigated by 3D finite element simulation. Three different cases, i.e. unclamped, clamped during welding and hot released immediately after welding, and clamped during welding and cold released after cooling down to ambient temperature, have been studied. Experiments have also been carried out for the unclamped case to measure temperature histories, residual stresses and angular distortions. According to the results of this study, the following conclusions are obtained:

- Clamping during welding and cold releasing after cooling to ambient temperature reduces final angular distortions, significantly.
- Clamping during welding and cold releasing after cooling to ambient temperature increases transverse residual stresses.
- Clamping during welding and cold releasing after cooling to ambient temperature increases longitudinal residual stresses at the bottom surface of the plate.
- Clamping during welding and hot releasing after welding does not affect the magnitude of deflections or residual stresses.

In summary, one can conclude that the final states of residual stresses and distortions strongly depend on the clamping time. Clamping during welding and cold releasing after cooling to ambient temperature has a significant effect on the reduction of angular distortions. This type of clamping could increase the residual stresses. On the contrary, clamping during welding and hot releasing after welding has very little effect on the reduction of angular distortions. This type of clamping does not affect the residual stresses. According to the results of this study, cold released clamping is suggested as a useful method to reduce angular distortions.

REFERENCES

1. Deng, D. and Murakawa, H. "Prediction of welding distortion and residual stress in a thin plate butt-welded joint", *Computational Materials Science*, **43**(2), pp. 353-365 (2008).
2. Long, H., Gery, D., Carlier, A. and Maropoulos, P.G. "Prediction of welding distortion in butt joint of thin plates", *Materials and Design*, **30**(10), pp. 4126-4135 (2009).
3. Deng, D. "FEM prediction of welding residual stress and distortion in carbon steel considering phase transformation effects", *Materials and Design*, **30**(2), pp. 359-366 (2009).
4. Chang, P.H. and Teng, T.J. "Numerical and experimental investigations on the residual stresses of the butt-welded joints", *Computational Materials Science*, **29**, pp. 511-522 (2004).
5. Camilleri, D., Comlekci, T. and Gray, T.G.F. "Computational prediction of out-of-plane welding distortion and experimental investigation", *The Journal of Strain Analysis for Engineering Design*, **40**(2), pp. 161-176 (2005).
6. Mollicone, P., Camilleri, D., Gray, T.G.F. and Comlekci, T. "Simple thermo-elastic-plastic models for welding distortion simulation", *Journal of Materials Processing Technology*, **176**(1-3), pp. 77-86 (2006).
7. Bachorski, A., Painter, M.J., Smailes, A.J. and Wahab, M.A. "Finite element prediction of distortion during gas metal arc welding using the shrinkage volume approach", *Journal of Materials Processing Technology*, **92-93**, pp. 405-409 (1999).
8. Michaleris, P. and Sun, X. "Finite element analysis of thermal tensioning technique mitigating weld buckling distortion", *Welding Journal*, **76**(11), pp. 451-457 (1997).
9. Deo, M.V. and Michaleris, P. "Mitigating of welding induced buckling distortion using transient thermal tensioning", *Science and Technology of Welding and Joining*, **8**(1), pp. 49-54 (2003).
10. Mochizuki, M. and Toyoda, M. "In-process control of welding distortion by reverse-side heating in fillet welds", *ASME, Pressure Vessels Piping Div. PVP*, **410**, pp. 29-36 (2000).
11. Seyyedian Choobi, M., Haghpanahi, M. and Sedighi, M. "Investigating the effect of welding sequence on angular distortions in butt welded plates", *IJW International Congress on Welding & Joining*, Tehran, Iran, pp. 143-150 (2009).
12. Deng, D. and Murakawa, H. "Numerical simulation of temperature field and residual stress in multi-pass welds in stainless steel pipe and comparison with experimental measurements", *Computational Materials Science*, **37**(3), pp. 269-277 (2006).
13. Goldak, J., Chakravarti, A. and Bibby, M. "A new finite element model for welding heat source", *Metallurgical and Materials, Transactions B*, **15**(2), pp. 299-305 (1984).
14. Messler, R.W., *Principles of Welding: Processes, Physics, Chemistry and Metallurgy*, John Wiley & Sons, Inc., Chapter 5, p. 136 (1999).

15. Lindgren, L.E. "Finite element modeling and simulation of welding part 1: Increased complexity", *Journal of Thermal Stresses*, **24**, pp. 141-192 (2001).
16. Seyyedian, M., Amini, Sh. and Haghpanahi, M. "Study of the effect of thickness on residual stresses in butt-welding of SUS304 plates", *IJW International Conference on Advances in Welding and Allied Technologies*, Singapore, pp. 195-200 (2009).
17. ASTM E837 "Standard test method for determining residual stresses by the hole-drilling strain-gauge method", in *Annual ASTM Book of Standards*, American Society for Testing and Materials, Philadelphia, Pennsylvania, USA (2004).
18. ANSYS User's Manual, ANSYS release 10.0., Swanson Analysis System, Houston (2006).

BIOGRAPHIES

Mahsa Seyyedian Choobi received a B.S. degree in Mechanical Engineering (Fluid Mechanics) from Tabriz University in 1998 and obtained a M.S. degree in Mechanical Engineering (Solid Mechanics) from Khaje Nassir-Al-Deen Toosi University of Technology (KNTU) in 2001. During her M.S. degree studies in KNTU, she participated in a research project in the field of developing a new method for cutting glass. Presently, she is a Ph.D. student in Mechanical Engineering (Solid Mechanics) at the Iran University of Science and Technology (IUST). Her Doctoral Thesis

M. Seyyedian Choobi, M. Haghpanahi and M. Sedighi

is in the field of Welding Residual Stresses and Distortions in Butt Welded Plates. She has published more than 15 papers in journals, and in international and national conference proceedings.

Mohammad Haghpanahi received a B.S. degree in Mechanical Engineering (Solid Mechanics) from Shiraz University of Technology. He continued his studies in Bio-Mechanical Engineering and obtained his M.S. and Ph.D. degrees from ENSAME University in France. Since 1990, he has been a faculty member in the Mechanical Engineering Department of the Iran University of Science and Technology (IUST). His fields of interest are: Bio-Mechanics, Vibration and Finite Element. He has published more than 120 papers in scientific journals and conference proceedings.

Mohammad Sedighi received a B.S. degree in Mechanical Engineering (Design and Manufacturing) from Sharif University of Technology. He continued his studies in Mechanical Engineering and obtained his M.S. and Ph.D. degrees from Bristol University in the United Kingdom. Since 1998, he has been a faculty member in the Mechanical Engineering Department of the Iran University of Science and Technology (IUST). His fields of interest are: Metal Forming, Modeling of Manufacturing Processes and Residual Stresses. He has published more than 110 papers in scientific journals and conference proceedings.